

Military Technical College
Kobry El-Kobbah,
Cairo, Egypt



9th International Conference
on Civil and Architecture
Engineering
ICCAE-9-2012

Experimental Study on the Behavior of Pile Group under Cyclic Lateral Loading

Mahmoud FawzyAwad-Allah*, Noriyuki Yasufuku, and Kiyoshi Omine*****

Abstract

Pile foundations supporting bridge piers, offshore platforms, and towers are required to resist not only static loading but also cyclic or dynamic lateral loading resulted from winds, sea waves, or earthquake actions. Therefore, it is necessary to examine the effects of slow cyclic loads on the pile foundation behavior. This paper presents an experimental study on pile models of different arrangements founded in both dense and loose sands of relative densities equal to $D_r=75\%$ and 35% , respectively. In this work, series of two-way lateral cyclic loading tests were performed on three pile arrangements (single, 3×1 , and 3×3 groups) having length to diameter ratio (L/d) of 10 and 20 with spacing to diameter ratio (S/d) of 3. The experimental setup was explained in details and the results were presented in the form of cyclic load–deflection curves and normalized bending moment charts against the number of cycles. Moreover, cyclic group efficiency, and cyclic p-multipliers were evaluated.

Keywords: Cyclic loading, experimental work, lateral deflection, sand, pile group, foundation.

1. INTRODUCTION

Pile foundations are widely used to support various structures such as offshore platforms, jetties, wharfs, docks, dolphin structures, and bridges. These structures are subjected to cyclic lateral loading due to wave and wind actions. In practice, however, after a foundation is constructed, it is quasi-statically loaded axially due to gravity loads of the superstructure. All cyclic loading sequences are characterized by four parameters, including: the maximum applied lateral load H_{max} , the number of cycles N , the frequency (rate of loading) f , and maximum lateral displacement y_{max} . Two-way cyclic loading can be considered as a simplified representation of dynamic loading without inertia nor damping. However, although alternating loading is symmetrical, the direction of the first loading remains in the pile memory (Rosquoet, 2007).

**Research Associate, National Research Center, Egypt, Tel: 0202-01006201192, Email: mahmoudfawzy1980@yahoo.com*

***Prof. of Geotechnical Engineering, Faculty of Engineering, Kyushu Univ., Japan, E-mail: Yasufuku@civil.kyushu-u.ac.jp*

****Asso. Prof. of Geotechnical Engineering, Faculty of Engineering, Kyushu Univ., Japan, Email: oomine@civil.kyushu-u.ac.jp*

The consideration of cyclic effects when designing piles is generally deduced from the soil-pile interactions under applied static loads using Winkler model. In the case of a linear elastic response of the soil-pile system, the soil reaction $P(z)$, at a depth z , depends on the modulus of soil reaction K_h , and on lateral displacement $y(z)$. Reese and Matlock (1956) suggest that K_h increases proportionally with z and soil reaction coefficient n_h as follows:

$$K_h = n_h z \quad (1)$$

Results from 34 full-scale cyclic lateral load tests of piles in sand were collected by Long and Vanneste (1994) to identify the factors affecting the cyclic behavior. These included soil density, pile type, installation method and, most importantly, the characteristics of the cyclic load. Long and Vanneste (1994) method is based on the deterioration of static “p-y” curves, which is taken into account by reducing the static soil reaction modulus according to:

$$K_h = N^{-t} n_h z \quad (2)$$

Where: t is a degradation factor that depends on the pile installation method, the load characteristics (one or two way loading), and on the relative density of sand.

An alternative method to model cyclic load effects, proposed by several authors, consists in reducing the soil reaction value by introducing a coefficient α as:

$$K_h = \alpha n_h z \quad (3)$$

Parakash (1961) suggests that $\alpha=0.7$ when the number of cycles N is less than 50. Broms (1964) proposes α equal to 0.75 and 0.50 for loose and dense sand, respectively, and $N=40$.

P-y reaction curves represent soil-pile interactions on the assumptions that the soil reaction, P , at all points of the pile is a nonlinear function of the lateral pile displacement. Different methods to determine the P-y curves can be found in the codes of practice such as API code (1993), P. H. R. I. (1980), and D. N. V. (1977). However, only the American and Norwegian technical specifications consider existence of the cyclic effects for designing piles subjected to lateral loads by introducing a reduction factor A on the ultimate soil reaction P_u , as given by Eq. 4.

$$P = AP_u \tan\left(\frac{n_h z}{AP_u} y\right) \quad (4)$$

Where: A is a factor to be considered for both monotonic loading ($A=0.9$) and cyclic loading ($A=3-0.8zd^{-1}$); P_u is ultimate soil reaction; and d is pile diameter.

However, although those reduction factors consider that the cycles affect surface layers ($z/d \leq 2.625$), API and DNV recommendations do not take into account the amplitude of the load and the number of cycles.

Rosauoet et al (2007) mentioned that frequency f , which has significant effects on time-dependent performances, does not influence the behavior of piles if they are constructed in dry sand. Therefore, it is necessary, in this paper, to examine the effects of dry sand and slow loading rate on the pile foundations behavior. This study is conducted to examine the effects of lateral cyclic loading on ultimate lateral pile capacity H_u , maximum mobilized bending moment, and P-y curves. In order to examine the behavior of piles under lateral cyclic loads, a new series of tests is carried out.

2. EXPERIMENTAL SETUP

2.1. Testing apparatus

Fig. 1 shows the laboratory test setup and the devices which are used for testing in the current experimental work. The model test facility consists of a medium size container of approximately wall thickness of 5 cm made of rigid fiberglass plates. The housing container has the following dimensions: 30 cm width by 95 cm length and 60 cm depth, resting on steel foundation. The container is placed inside a loading steel frame constructed to support the loading actions during applying the horizontal loads. The loading system is designed to be rigid and capable of sustaining the loading stresses without suffering from deflection. Fig. 2 depicts the loading system, data logger, and external control unit devices which are used to record data and control the number of applied cycles during testing.

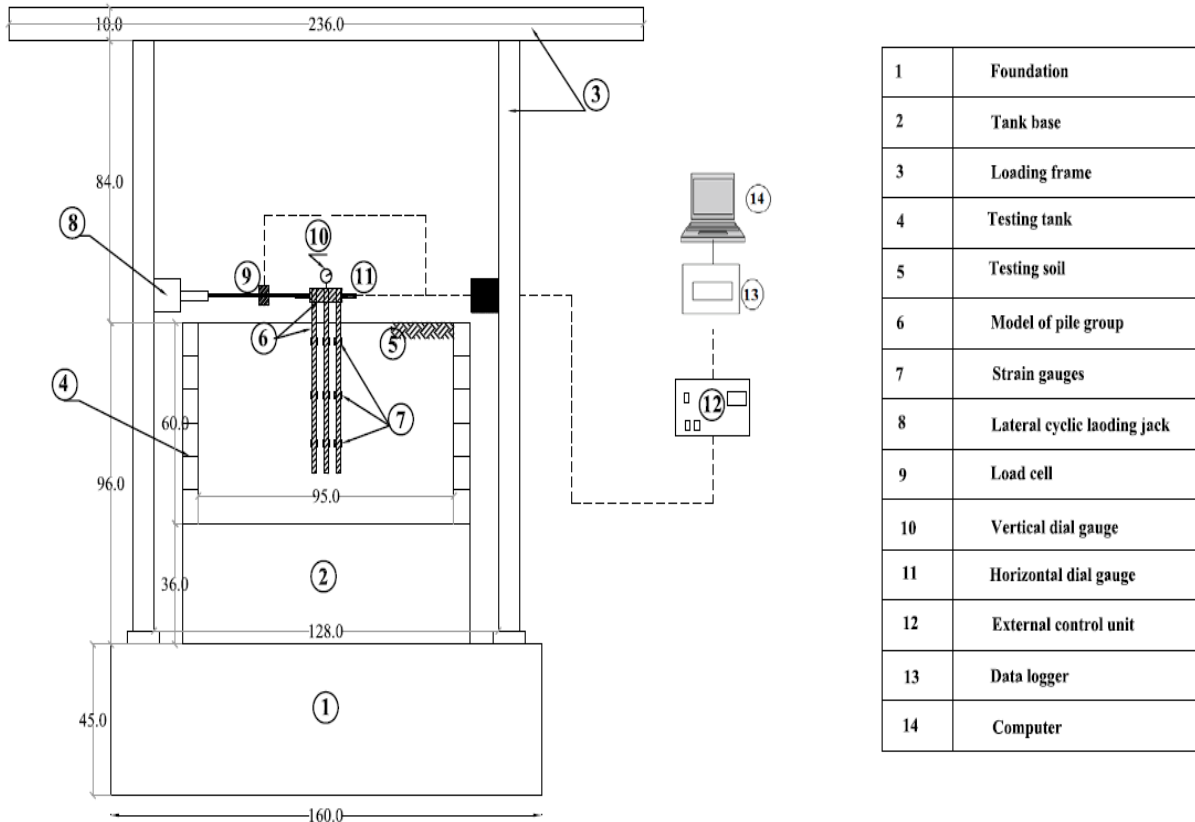


Fig. 1. Experimental setup (dimensions in cm)

2.2. Pile model

The pile models are manufactured from closed-end aluminum alloy 6061 tube of outer diameter of 15mm and wall thickness of 1.5mm (Fig. 3). The young's modulus of the used aluminum alloy is $70 \times 10^9 \text{ KN/m}^2$. Aluminum plates of 6mm thick are used as pile caps which are attached at the top of piles leaving 60mm above the ground surface as free standing length for the ground. Screwing of piles in the holes provided in the pile cap of depth 40mm leads to partial fixation condition. To increase the pile wall friction angle, sand was added around the pile by adhesives.

Equivalence law is used adhered to when designing the model pile material, dimensions, and the applied speed and displacement. The following scaling formula proposed by Wood et al. (2002) is employed in this research:

$$\frac{E_m I_m}{E_p I_p} = \frac{1}{n^5} \tag{5}$$

Where: E_m is modulus of elasticity of model pile; E_p is modulus of elasticity of prototype pile; I_m is moment of inertia of model pile; I_p is moment of inertia of prototype pile; and n is scale factor for length.

In the experimental work, the scaling factor for length is adopted as $n=20$; therefore the value of scaling factor for pile rigidity will be equal to $(1/n=1/20^5)$. Hence, if an aluminum tube pile model of outer diameter 15mm and wall thickness 1.5mm is used, it will be equivalent to a prototype of circular steel pile of outer diameter 0.61m and wall thickness of 2cm. Similarly, the actual wave and wind speeds were simulated in the laboratory using scaling factor $n=10$, which means that when the applied laboratory lateral speeds are equal to 0.2, 0.4, and 0.6 mm/s, the corresponding in-situ wind and wave speeds will be equivalent to 20, 40, and 60m/s, respectively.

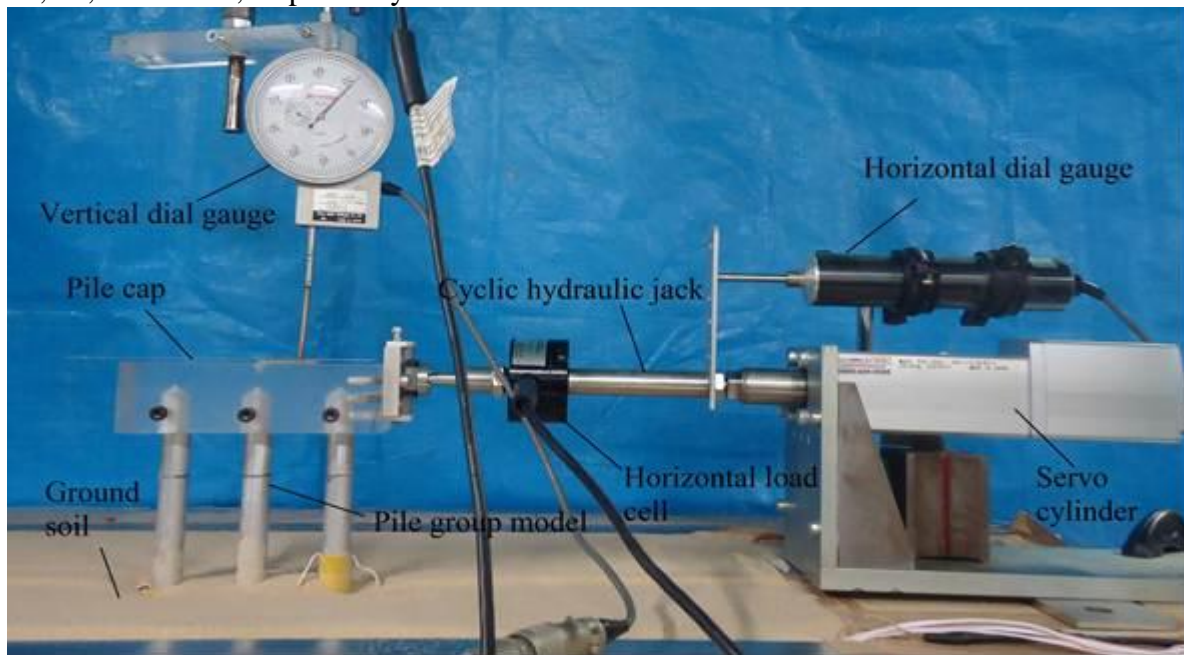


Fig. 2. Horizontal cyclic loading system and measuring apparatus, data logger, and external control unit



Fig. 3. Single pile model attached strain gauges

Fig. 4 illustrates the cyclic loading pattern of lateral load applied on the pile model during testing program. Two-way symmetric cyclic lateral load is imposed horizontally on two opposite sides of pile cap model to provide horizontal deflection of 3 mm (20% of pile diameter) at pile cap in each side. Cyclic lateral load is applied for 1, 2, and 3 cycle per minute (cpm) so that it generally can simulate the impact of the wave loading of storm waves in most of costal regions. Cyclic horizontal load is applied for 50 cycles in all experiments. The bending moment, horizontal displacement, vertical settlement, and earth pressure, which were obtained from loading action, were measured and recorded during test performance.

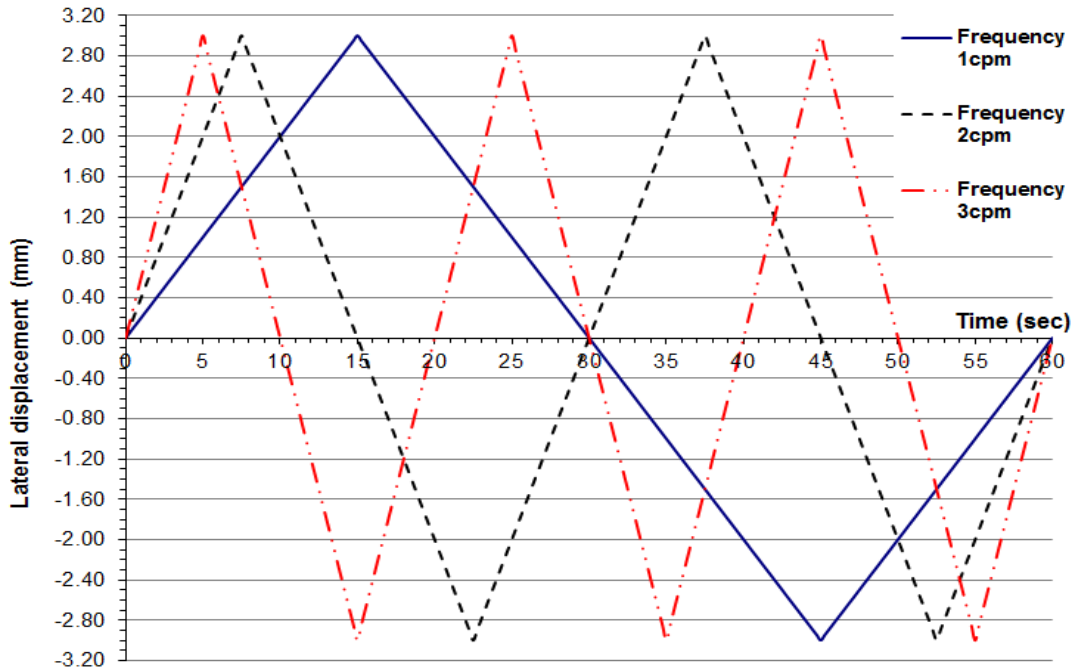


Fig. 4. Typical cyclic loading pattern

2.3. Preparation of testing soil

The testing soil, used in this laboratory work, is sub-angular, fine Toyoura sand, which is commonly used sand in Japan, and its index properties are given in Table 1. $G_s = 2.65$. In this study, two different states of relative densities (D_r) are considered, including loose and dense sand of 35% and 75%, respectively. Relative density values will be achieved during testing program procedures using especial compaction tool known as multiple sieving pluviation (MSP) method (Miura and Toki, 1982) which is explained in the next section.

2.3.1. Multiple sieving pluviation (MSP) method

Miura and Toki (1982) introduced a method for preparation of sand samples using multiple sieving pluviation apparatus (Fig. 5a) by controlling the rate of sand discharge. Using this method, the loose and dense sand of relative densities of 35% and 75% have been achieved, respectively, without applying vibration or impact. The rate of sand discharge can be controlled by height of fall and nozzle diameter as shown in Fig. 5b.

Table 1. Geotechnical properties of Toyoura sand

| Description | Value |
|------------------------------------|------------------------|
| Specific gravity (G_s) | 2.65 |
| Maximum density (γ_{max}) | 16.0 kN/m ³ |
| Dry density (γ_{dry}) | 13.1 kN/m ³ |
| Maximum void ratio (e_{max}) | 0.98 |

| | |
|----------------------------------|--------|
| Minimum void ratio (e_{min}) | 0.62 |
| Uniformity coefficient (U) | 1.40 |
| Coefficient of curvature (C) | 0.86 |
| Effective diameter (D_{50}) | 0.18mm |

3. TEST PROCEDURES AND CONFIGURATIONS

The testing tank is cleaned up to make sure that it is free from any impurities or debris. The pile model is placed at the center of the testing tank by clamping it against the guide bar to avoid boundary effects, meanwhile examination of its vertical alignment is performed. Then, sand is poured in carefully, slowly, and evenly layers of 10 cm in thickness using the previously described method (Miura and Toki, 1982). After reaching to the uppermost layer of sand, the guide beam is removed and the top surface is flattened. Three different model pile arrangement patterns are chosen to be used in the experimental testing program namely, single, grouped pile of 3x1 and 3x3. Furthermore, two length to diameter (L/d) ratios of model pile are selected to be tested including, 10, and 20 which are equivalent to prototype dimensions of 6.1m, and 12.2m. The spacing among piles in grouped piles is maintained constant, being equal to 3d in both of direction of loading vector and perpendicular direction. The detailed conducted test program (36 tests) is represented in Table 2 together with the associated test condition.



Fig 5a. Multiple sieving pluviation apparatus

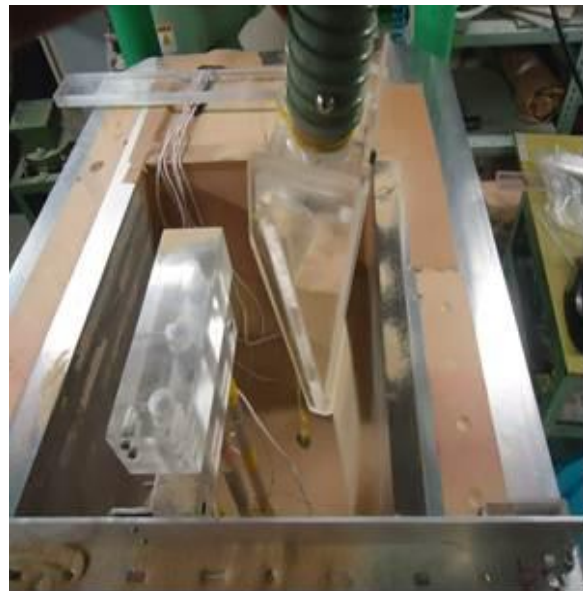


Fig 5b. Nozzle size and falling of sand from fixed height

4. ANALYSIS OF THE RESULTS

4.1. Vertical settlement

During applying lateral cyclic loading, vertical settlement at pile head was detected using vertical dial gauge as shown in Fig.2. Normalized vertical settlement, which is defined as the measured settlement (s_m) to 10% of pile diameter settlement (s_o), is plotted against the number of cycles N for loose and dense sand (Fig. 6 and Fig.7). It is noticeable that these relationships are nonlinear. It can be seen that by increasing the number of cycles the single piles sink into soil. The single piles, which are subjected to high frequency ($f=3\text{cpm}$), sink deeper in soil, and this occurs at number of cycles between 0 and 25, which means that although the piles are in dry sand, they are significantly affected by the slow frequency of loading. Moreover, single pile of L/d of 10 settles into soil faster than single pile of L/d ratio of 20. It is important to

mention that dense and loose soils give relatively similar patterns of relationships under the same number of cycles.

For pile groups, the relationships between the normalized settlement and number of cycles are different from those of single piles, since at less much number of cycles ($N < 10$) upward movement has been observed; this behavior is mostly apparent in pile group of L/d ratio of 10. This phenomenon can be attributed to that confining pressure increases during cyclic loading, especially for pile groups, which causes higher confining pressure inside pile groups, as a result upward movement happens after about 10 and 20 cycles for dense and loose sand, respectively.

Table 2. Total number of experimental tests and associated test conditions

| Dense sand | | | | | | Loose sand | | | | | |
|------------|-------------------------------------|--------------------------|-----|------|--------------------------------|------------|-------------------------------------|--------------------------|-----|------|--------------------------------|
| Test ID | Relative density (D _r %) | Pile arrangement pattern | L/d | S/d | Test characteristics | Test No. | Relative density (D _r %) | Pile arrangement pattern | L/d | S/d | Test characteristics |
| 1 | 75 | Single | 10 | ---- | Cyclic (N= 0 to 50), f(cpm)= 1 | 19 | 35 | Single | 10 | ---- | Cyclic (N= 0 to 50), f(cpm)= 1 |
| 2 | 75 | Single | 10 | ---- | Cyclic (N= 0 to 50), f(cpm)= 2 | 20 | 35 | Single | 10 | ---- | Cyclic (N= 0 to 50), f(cpm)= 2 |
| 3 | 75 | Single | 10 | ---- | Cyclic (N= 0 to 50), f(cpm)= 3 | 21 | 35 | Single | 10 | ---- | Cyclic (N= 0 to 50), f(cpm)= 3 |
| 4 | 75 | Single | 20 | ---- | Cyclic (N= 0 to 50), f(cpm)= 1 | 22 | 35 | Single | 20 | ---- | Cyclic (N= 0 to 50), f(cpm)= 1 |
| 5 | 75 | Single | 20 | ---- | Cyclic (N= 0 to 50), f(cpm)= 2 | 23 | 35 | Single | 20 | ---- | Cyclic (N= 0 to 50), f(cpm)= 2 |
| 6 | 75 | Single | 20 | ---- | Cyclic (N= 0 to 50), f(cpm)= 3 | 24 | 35 | Single | 20 | ---- | Cyclic (N= 0 to 50), f(cpm)= 3 |
| 7 | 75 | 3x1 group | 10 | 3 | Cyclic (N= 0 to 50), f(cpm)= 1 | 25 | 35 | 3x1 group | 10 | 3 | Cyclic (N= 0 to 50), f(cpm)= 1 |
| 8 | 75 | 3x1 group | 10 | 3 | Cyclic (N= 0 to 50), f(cpm)= 2 | 26 | 35 | 3x1 group | 10 | 3 | Cyclic (N= 0 to 50), f(cpm)= 2 |
| 9 | 75 | 3x1 group | 10 | 3 | Cyclic (N= 0 to 50), f(cpm)= 3 | 27 | 35 | 3x1 group | 10 | 3 | Cyclic (N= 0 to 50), f(cpm)= 3 |
| 10 | 75 | 3x1 group | 20 | 3 | Cyclic (N= 0 to 50), f(cpm)= 1 | 28 | 35 | 3x1 group | 20 | 3 | Cyclic (N= 0 to 50), f(cpm)= 1 |
| 11 | 75 | 3x1 group | 20 | 3 | Cyclic (N= 0 to 50), f(cpm)= 2 | 29 | 35 | 3x1 group | 20 | 3 | Cyclic (N= 0 to 50), f(cpm)= 2 |
| 12 | 75 | 3x1 group | 20 | 3 | Cyclic (N= 0 to 50), f(cpm)= 3 | 30 | 35 | 3x1 group | 20 | 3 | Cyclic (N= 0 to 50), f(cpm)= 3 |
| 13 | 75 | 3x3 group | 10 | 3 | Cyclic (N= 0 to 50), f(cpm)= 1 | 31 | 35 | 3x3 group | 10 | 3 | Cyclic (N= 0 to 50), f(cpm)= 1 |
| 14 | 75 | 3x3 group | 10 | 3 | Cyclic (N= 0 to 50), f(cpm)= 2 | 32 | 35 | 3x3 group | 10 | 3 | Cyclic (N= 0 to 50), f(cpm)= 2 |
| 15 | 75 | 3x3 group | 10 | 3 | Cyclic (N= 0 to 50), f(cpm)= 3 | 33 | 35 | 3x3 group | 10 | 3 | Cyclic (N= 0 to 50), f(cpm)= 3 |
| 16 | 75 | 3x3 group | 20 | 3 | Cyclic (N= 0 to 50), f(cpm)= 1 | 34 | 35 | 3x3 group | 20 | 3 | Cyclic (N= 0 to 50), f(cpm)= 1 |
| 17 | 75 | 3x3 group | 20 | 3 | Cyclic (N= 0 to 50), f(cpm)= 2 | 35 | 35 | 3x3 group | 20 | 3 | Cyclic (N= 0 to 50), f(cpm)= 2 |
| 18 | 75 | 3x3 group | 20 | 3 | Cyclic (N=0 to 50), f(cpm)= 3 | 36 | 35 | 3x3 group | 20 | 3 | Cyclic (N=0 to 50), f(cpm)= 3 |

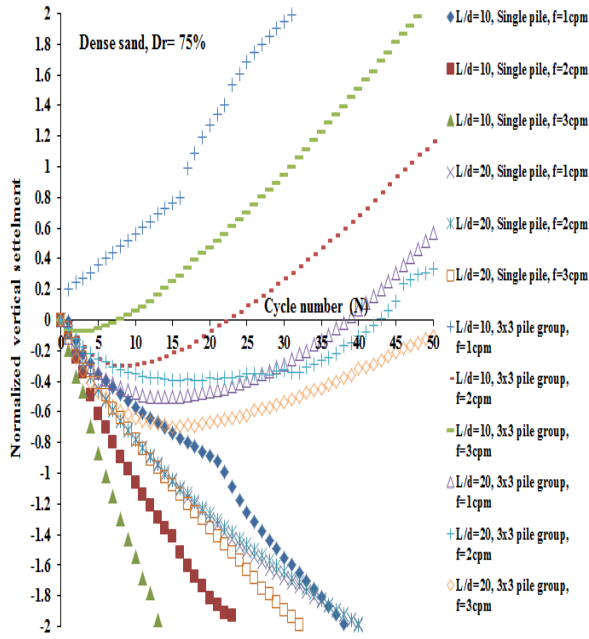


Fig. 6 Normalized vertical settlement versus number of cycles for piles in dense sand

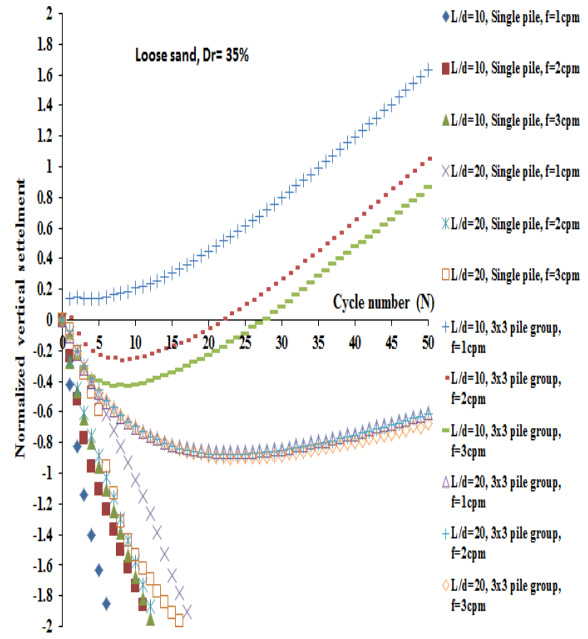


Fig. 7 Normalized vertical settlement versus number of cycles for piles in loose sand

4.2. Maximum mobilized bending moment

From an engineering point of view, the maximum bending moment, in most cases, is considered as the key parameter as regards laterally loaded pile design. This section presents the main experimental results concerning pile bending moment measurements as a function of depth directly deduced through a preliminary calibration from the 6 pairs of strain gauges mounted along the model pile (Fig. 3).

The evolution of the normalized bending moment (M_m/M_y), which is the ratio of maximum measured bending moment at cycle N to the moment that causes yield of pile material, is shown in Figs. 8 and 9. The bending moment is calculated from the bending strain measured at various points along the length of the instrumented model piles using the following expression:

$$M_m = EI\varepsilon / r \tag{6}$$

Where: E= Young’s modulus of the model pile material, I= moment of inertia of the model pile, ε = measured bending strain and r = horizontal distance between strain gauge position (outer surface of the pile) and neutral axis.

The yielding moment (M_y) of the pile model is calculated the using the following expression (σ_y = yield stress of pile material):

$$M_y = \sigma_y I / r \tag{7}$$

Figs. 8 and 9 illustrate that the larger of both of L/d ratio and number of cycles N are, the higher the normalized bending moment is, which means that the L/d and N control the mobilization of maximum bending moment of single and grouped piles rather than the frequency of loading. It is also significant to notice that the majority of growth in normalized bending moment has occurred in the initial ten cycles of loading (i.e. N=10), but a little increasing in normalized bending moment happened during the remaining cycles. However, to a lesser extent, soil relative density has a little impact on mobilization of maximum bending moment since variation in bending moment values are not quite large. Furthermore, it is

worthy to notice that none of tests exceeds normalized bending moment value of 1 because all tests are conducted under slow lateral cyclic loading.

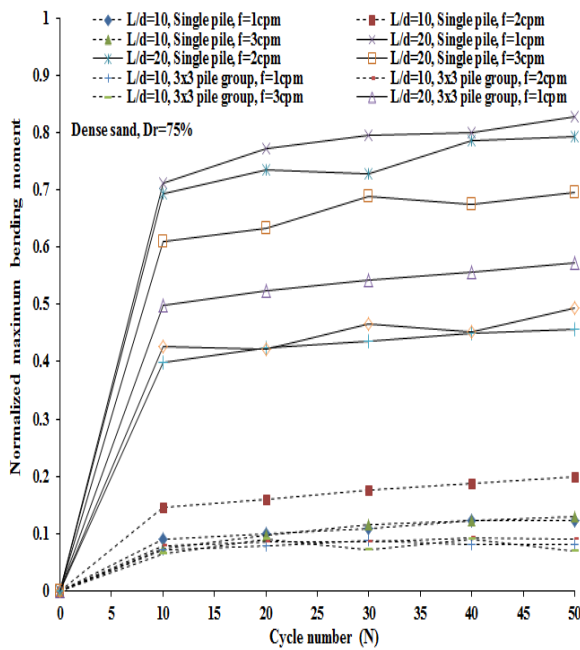


Fig. 8 Normalized bending moment versus number of cycles for piles in dense sand

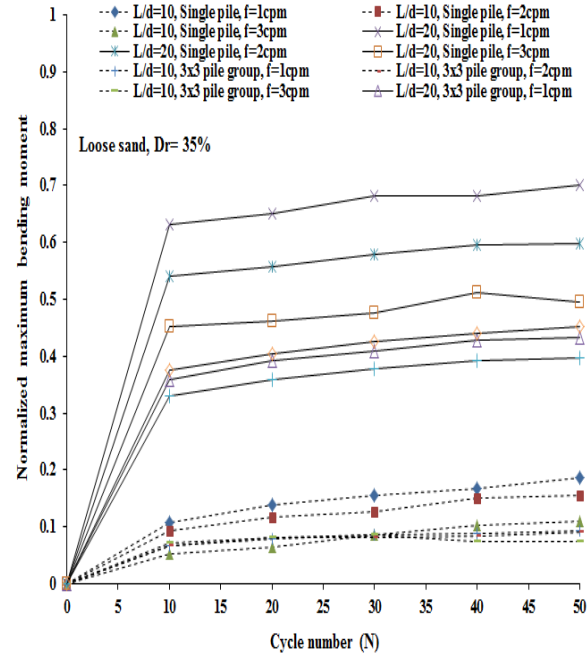


Fig. 9 Normalized bending moment versus number of cycles for piles in loose sand

Additionally, Figs. 10 and 11 depict the relationships between the maximum normalized bending moment values of trailing and leading piles in grouped piles at number of cycles N of 5, 30, and 50 and the rate of loading f of 1, 2, and 3 cpm for dense and loose sand, respectively. Table 3 shows the values of the maximum normalized bending moment of trailing and leading piles in grouped piles for dense and loose sand along with the percent of variation of mobilized bending moment at number of cycles 5, 30, 50. The percentages of variations in maximum bending moment are between 22.8% and 45.6% for piles in dense sand, and between 23.5% and 53.9% for piles in loose sand.

Furthermore, even if the lateral cyclic loading is constant and identical in both directions during load application, the values of normalized bending moments of leading piles are almost higher than those of trailing ones. This phenomenon is known as shadowing effect in which the soil resistance of a pile in a trailing row is reduced because of the existence of the leading pile ahead of it (Fig. 12). The shadowing effect makes the stress zone out of a pile and the surrounding soils can produce a passive wedge along the pile. This wedge will interact with others and then reduce the soil resistances. In consequence, the soils along the trailing piles would be more significantly affected than those along the leading piles; individual pile loads are thus different (Chang et al., 2009).

4.3. Cyclic P-y curve

The soil-structure interaction model is classically used to design laterally loaded piles. This model, which requires the knowledge of the P-y curves, is based on the elastic beam theory to determine the pile lateral displacement and the bending moment. A similar method is used for the interpretation of the experimental results.

The bending moment along the length of the pile at discrete points calculated using Eq. 6 is analyzed using curve fitting involving a fifth order polynomial. The soil reaction (P) is determined by double differentiation and pile deflection (y) is obtained by double integration

of moment curves. The boundary conditions adopted to solve the equations are the measured pile head deflection and zero deflection at pile tip (Chandrasekaran et al, 2010).

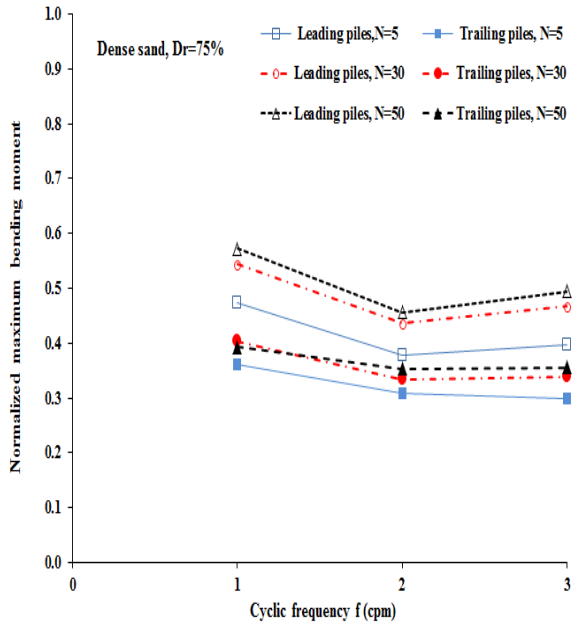


Fig. 10 Relationships between normalized bending moment and cyclic frequency at different cycle numbers for dense sand

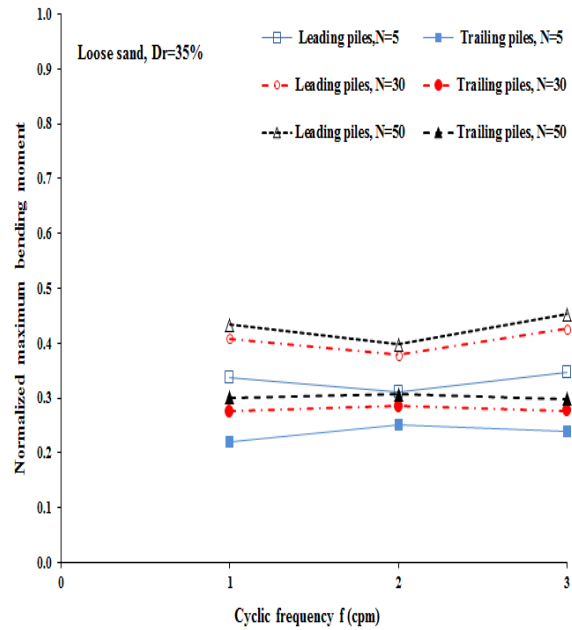


Fig. 11 Relationships between normalized bending moment and cyclic frequency at different cycle numbers for loose sand

Table 3 Percent of variation of normalized bending moment of leading and trailing piles

| Frequency f (cpm) | Cycle number | Dense sand | | | loose sand | | |
|-------------------|--------------|---|----------------|------------------------|---|----------------|------------------------|
| | | Maximum normalized bending moment M_m/M_y | | | Maximum normalized bending moment M_m/M_y | | |
| | | Leading piles | Trailing piles | Percent of variation % | Leading piles | Trailing piles | Percent of variation % |
| 1 | N = 5 | 0.473 | 0.361 | 31.0 | 0.337 | 0.220 | 53.0 |
| 2 | | 0.378 | 0.308 | 22.8 | 0.310 | 0.251 | 23.5 |
| 3 | | 0.398 | 0.300 | 32.7 | 0.347 | 0.240 | 45.4 |
| 1 | N = 30 | 0.543 | 0.404 | 34.4 | 0.408 | 0.275 | 48.4 |
| 2 | | 0.435 | 0.334 | 30.3 | 0.379 | 0.285 | 32.9 |
| 3 | | 0.467 | 0.339 | 37.9 | 0.426 | 0.277 | 53.9 |
| 1 | N = 50 | 0.572 | 0.393 | 45.6 | 0.434 | 0.301 | 44.3 |
| 2 | | 0.456 | 0.353 | 29.2 | 0.397 | 0.307 | 29.6 |
| 3 | | 0.494 | 0.356 | 38.7 | 0.452 | 0.298 | 51.9 |

Note: Percent of variation = $100 * [(M_m - M_y)_{\text{leading}} - (M_m - M_y)_{\text{trailing}}] / (M_m - M_y)_{\text{trailing}}$

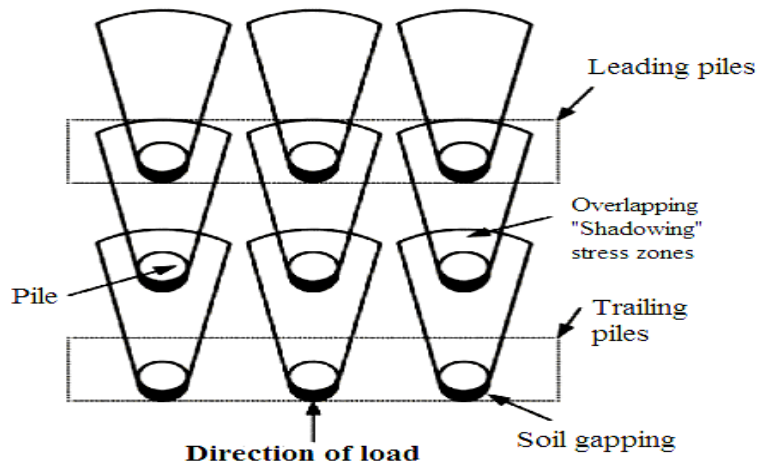


Fig. 12 Shadowing effect of laterally loaded pile foundation

Fig.13 indicates that, at shallow depths ($z < 6d$), load cycles and frequencies cause a raise of soil reaction, P , since by increasing the rate of loading and number of cycles, an obvious increase in both of soil reaction and lateral displacement are observed. On the other hand, Fig. 14 indicates that, at deeper depths ($z > 15d$), a reduction in the soil resistance and lateral displacement are observed due to increase of cyclic loading and frequencies. Accordingly, development of P - y curves does not only depend on soil properties, as given in Eq. 4, but also the rate of loading, f , and number of cycles, N . Consequently, for piles constructed in dry sandy soil and subjected to cyclic loading, it can be seen that at small depths soil softening occurs while at deep depths soil hardening occurs. Therefore, from geotechnical point of view, the top layers (i.e. within $z < 6d$) governs the design and analysis of piles under applied lateral loads since the soil reactions mobilized in these layers control the behavior. But, due to the flexible piles used in the present study, the contribution of deep layers in the pile equilibrium is not significant.

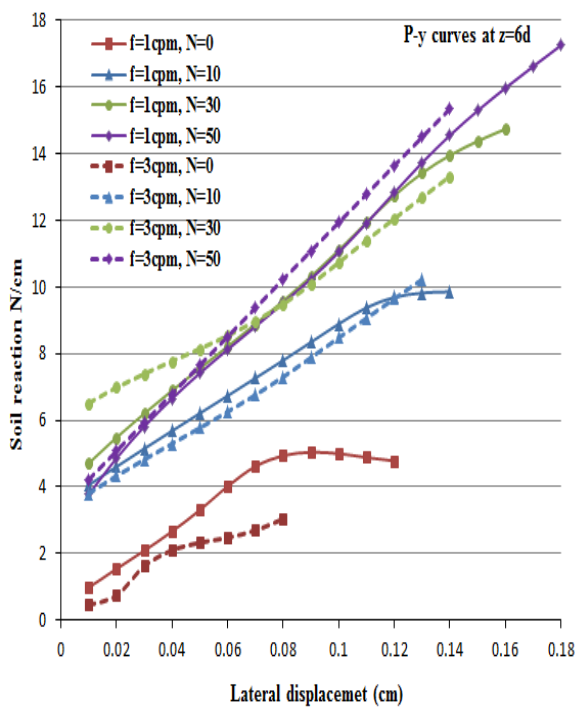


Fig. 13 Cyclic P - y curves at depth $6d$ for piles in dense sand ($D_r=75\%$)

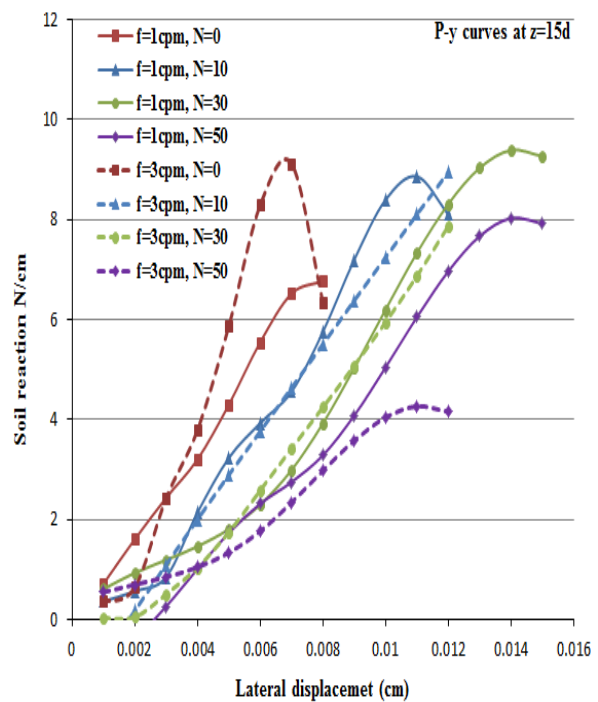


Fig. 14 Cyclic P - y curves at depth $10d$ for piles in dense sand ($D_r=75\%$)

4.4. Lateral load-displacement curve

The collection of both the applied lateral load H and the pile head displacement y_H , using manufactured load cell is easy. The incremental ratio gives the tangent stiffness modulus K of the system.

Typical results of monotonic (i.e. initial loading $N=0$) and cyclic tests are given in Figs. 15 and 16 for dense and loose sand, respectively, and the cyclic loading is performed to 50 two-way cycles. It can be noticed that, first loading cycle (monotonic test) generates a lower lateral ultimate load than the following ones. The tangent stiffness related to the first cycle is lower than those related to cyclic phase. The stiffness increases with the number of cycles, N , tending then towards a maximum value.

This phenomenon can be owned to one of the following reasons: (1) cyclic loading leads to hardening of sandy soil and reduction of void ratio. Consequently, enhancement of soil properties occurs for loose sand occurs; (2) Confining pressure increases during cyclic

loading, especially for pile groups, which causes higher confining pressure inside pile groups, as a result upward movement happens after about 10 and 20 cycles for dense and loose sand, respectively.

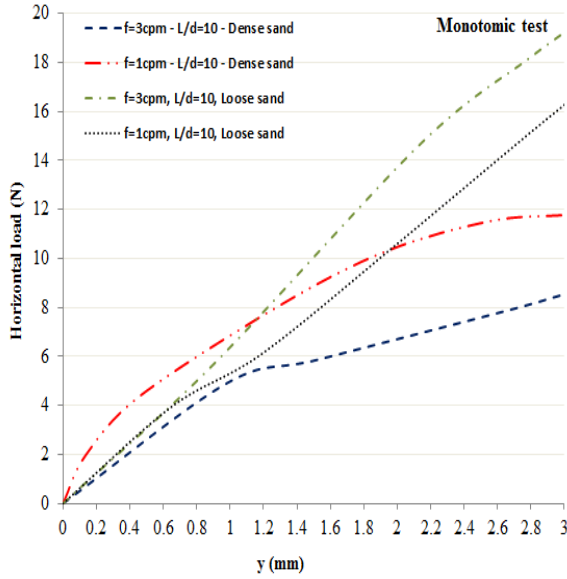


Fig. 15 Load versus lateral displacement curves for single short piles in dense and loose soils

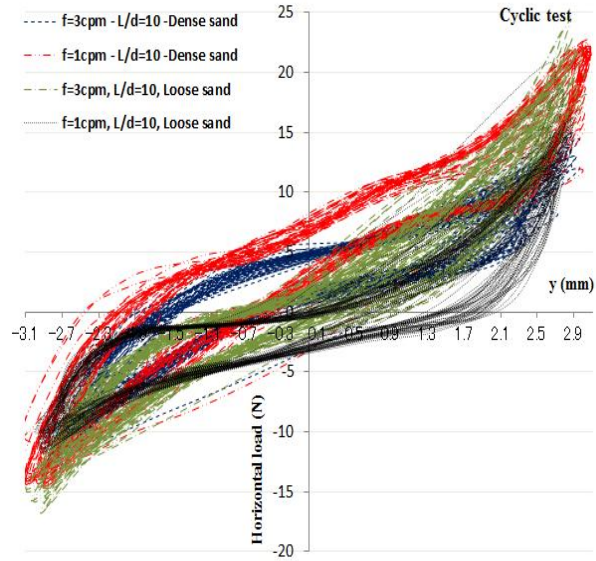


Fig. 16 Cyclic load-lateral displacement curves for single short piles in dense and loose soils

4.5. Cyclic P-multiplier (r)

Cyclic P-multipliers, r, are evaluated by comparing the ultimate soil resistance at different cycles numbers (N=10, 30, and 50) with that of the single pile under static loading (N=0). The cyclic P-multipliers are evaluated for single piles subjected to frequencies of 1cpm to 3cpm, and the number of cycles is maintained to 50 cycles (severe conditions). Table 4 gives the values of cyclic P-multipliers for piles in dense sand layers. Cyclic P-multipliers are calculated using Eq. 8:

$$r = \frac{P_m - P_c}{P_c} \quad (8)$$

Where: P_m = soil reaction mobilized during monotonic test, and P_c = soil reaction mobilized during cyclic test. The negative values imply that, r, are degraded, and positive values denote that, r, are evolved.

It is obvious that the cyclic P-multipliers (r) are markedly affected by the loading frequency and the number of cycles. For the layers at depths of 3d to 6d from ground level, P-multipliers increase with increasing the number of cycles and loading frequencies. On contrast, for the layers at depths of 10d to 15d from ground level, reduction of cyclic P-multipliers (r) occurs since cyclic P-multipliers reduce with increasing the number of cycles and loading frequencies.

Table 4 Values of P-multipliers mobilized in dense sand layers along pile length

| Depth of layer | Loading frequency | Cyclic P-multipliers (r) | | | Loading frequency | Cyclic P-multipliers (r) | | |
|----------------|-------------------|--------------------------|-------|-------|-------------------|--------------------------|-------|-------|
| | | N=10 | N=30 | N=50 | | N=10 | N=30 | N=50 |
| Z=3d | 1cpm | 0.89 | 0.95 | 0.95 | 3cpm | 0.51 | 0.47 | 0.46 |
| Z=6d | | 0.50 | 0.59 | 0.58 | | 0.67 | 0.77 | 0.75 |
| Z=10d | | -0.25 | -0.54 | -0.43 | | -0.21 | -0.27 | -0.26 |
| Z=15d | | -0.82 | -0.98 | -2.65 | | -0.91 | -2.21 | -2.39 |

Note: $r = (P_m - P_c) / P_c$

4.6. Cyclic group efficiency (G_c)

In the field, piles are often arranged in groups, and the behavior of a pile group may differ substantially from that of a single pile. Mandolini et al. (2009) reported that the response of a laterally loaded pile group with relatively closely spaced piles is quite different from that of a single pile due to the following reasons: (1) Interaction between piles through the surrounding soil; (2) Rotational restraint exerted by the cap connecting the piles at the head; (3) Additional resistance to lateral load provided by frictional resistance at the cap-soil interface; and (4) Passive resistance results from totally or partially embedment of structure.

Group efficiency is calculated depending on the number of piles in a group and the layout of the group, as given in Eq. 9:

$$G_c = \frac{H_g}{n * H_s} \tag{9}$$

Where: H_g = total horizontal load applied to the group; H_s = horizontal load carried by a single pile at the same horizontal displacement; and n = number of piles in the group.

Figs. 17 and 18 depict the relationship between the cyclic group efficiency (G_c) and loading frequencies (f) at wide range of number of cycles (N) for grouped piles of 3x1 and 3x3 embedded in loose and dense sandy soil. It has been noticed that those relationships are nonlinear. Furthermore, the efficiency of a pile group reduced with the increase in number of piles in the group since the G_c for 3x3 grouped pile are ranged from 0.45 to 0.49 and from 0.27 to 1.42, whereas for 3x1 grouped pile are ranged from 0.81 to 0.5 and from 0.43 to 2.34 for dense and loose sand, respectively. This can be due to the increased number of overlapping zones of passive and active wedges.

Fig. 17 indicates that the cyclic group efficiency increases with increasing the loading frequencies and the number of cycles for piles of L/d equal 20 installed in dense sand ($D_r=75\%$). Fig. 18, however, shows that with increasing the loading frequencies and the number of cycles, reduction of cyclic group efficiency reduces significantly, for piles of L/d equal 10 installed in loose sand ($D_r=35\%$).

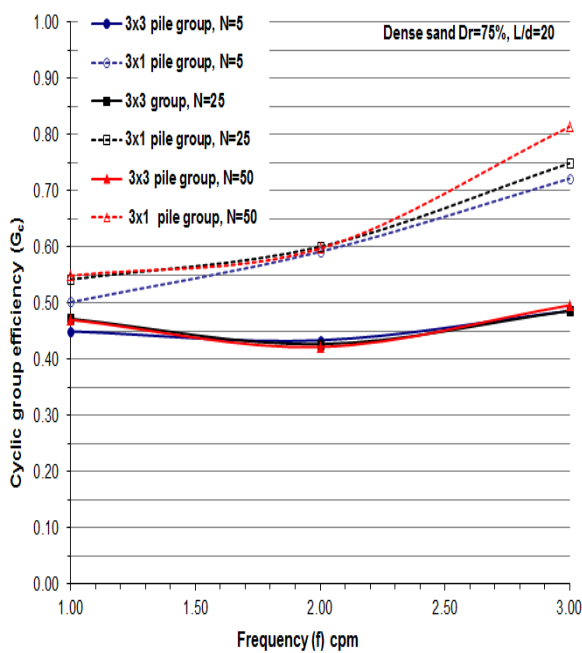


Fig. 17 Relationship between G_c and f at different number of cycles N for grouped piles of $L/d=20$ embedded in dense sand

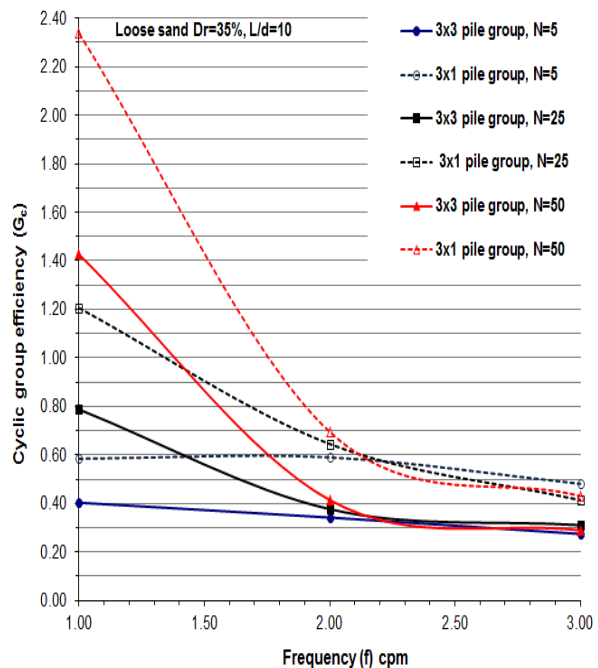


Fig. 18 Relationship between G_c and f at different number of cycles N for grouped piles of $L/d=10$ embedded in loose sand

5. SUMMARY AND CONCLUSION

This paper presents a comprehensive investigation carried out on pile foundations (i.e. single and grouped piles) embedded in dry Toyoura sand, which is a typical testing material used for geotechnical experimental work in Japan, under lateral cyclic loading. Additionally, this study aims to study the effects of number of cycles of loading, loading frequencies, L/d and size of the group on the load-deflection and bending behavior of pile. The experimental results are used to develop the cyclic P-multipliers. The conclusion of this study can be summarized as follows:

- 1) Single piles embedded in dry sand are markedly affected by the slow frequency of loading (i.e. $f = 1, 2, \text{ and } 3$ cpm). For grouped piles, the relationships between the normalized settlement and number of cycles are different from those of single piles, since upward movement has been observed at low number of cycles ($N < 10$); this behavior is mostly apparent in pile group of L/d ratio of 10.
- 2) L/d and N control the mobilization of maximum bending moment of single and grouped piles rather than f . Moreover, the majority of the progress in normalized bending moment happens in the initial 10 cycle of loading, however, a slight increasing in normalized bending moment occurred during the remaining 40 cycles.
- 3) The phenomenon of shadowing effect has been observed during applying lateral cyclic loading although the lateral cyclic loading is constant and equal in both directions during load application. The percentages of variations in maximum bending moment are between 22.8% and 45.6% for piles in dense sand, and between 23.5% and 53.9% for piles in loose sand. Therefore, this effect has to be considered in design.
- 4) Evolution of P-y curves does not only based on soil properties, as given in the codes of practice such as API code (1993), P. H. R. I. (1980), and D. N. V. (1977), but also the rate of loading, f , and number of cycles, N .
- 5) Cyclic P-multipliers (r) are obviously influenced by the loading frequency and the number of cycles where in shallow layers at depth from 3d to 6d, cyclic P-multipliers increase with increasing the number of cycles and loading frequencies. On contrarily, in deep layers at depths of 10d to 15d, reduction of cyclic P-multipliers (r) occurs with increasing the number of cycles and loading frequencies.
- 6) Likewise, cyclic group efficiency (G_c) is noticeable affected by increase in loading frequencies and number of cycles for grouped piles of L/d equal 20 installed in dense sand ($D_r = 75\%$) and for those of L/d equal 10 installed in loose sand ($D_r = 35\%$) as well.

REFERENCES

- American Petroleum Institute (API). 1993. "Designing and constructing fixed offshore platforms." RP2A-LRFD, Session G, Washington, D.C., pp. 64–77.
- Broms, B. B. 1964. "Lateral Resistance of Piles in Cohesionless Soils." *Journal of Soil Mechanics and Foundation Division, ASCE*, Vol. 90, No. SM3, pp. 123-156.
- Chandrasekaran, S. S. Boominathan, A. and Dodagoudar, G. R. 2010. "Experimental investigations on the behavior of pile groups in clay under lateral cyclic loading." *Springer, GeotechGeolEng*, Vol. 28, No. 5. pp. 603-617.
- Chang D.W, Bor-Shiun Lin, and Shih-Hao Cheng. 2009. "Lateral load distributions on grouped piles from dynamic pile-to-pile interaction factors." *Int J for Numerical and Analytical Methods*, Vol. 33, pp. 173–191.
- D. N. V.-Det Norske Veritas 1977. "Rules for the design construction and inspection of offshore structures." Appendix F, Foundations, 5 p.
- Long, J. H., and Vanneste, G. 1994. "Effects of cyclic lateral loads on piles in sand." *ASCE Journal of Geotechnical Engineering*, Vol. 120, No. 1, pp. 225-243.
- Mandolini, A., Russo, G., and Viggiani, C. 2009. "Pile foundations: experimental investigation, analysis and

- design.” State of the Art Report.Proc.Of 16th Int. Conf. on Soil Mechanics and Geotechnical Engineering, Osaka. Vol. 1, 177-213.
- Miura, S., and Toki, S. 1982. “A simple preparation method and its effect on static and dynamic deformation-strength properties of sand.” *Soils and Foundations*, Vol.22, No. 1, pp. 61-77.
- P. H. R. I.-Port and Harbor ResearchInstitute 1980. “Technical standards for port and harbor facilities in Japan.” Office of ports and harbor,Ministry of Transportation, 317 p.
- Prakash, S. 1961. “Behavior of piles groups subjected to lateral loads, Thesis, University of Illinois, Urbana, III, 218p.
- Reese, L. C. and Matlock, H. 1956. “Non-dimensional solution for laterally loaded in sand.” Paper No. 2080, 6th Annual Offshore Tech. Conf., 2, Houston, Texas.
- Rosquoet, F., Thorel, L., Garnier, J., and Canepa, Y. 2007. “Lateral cyclic loading of sand-installed piles.” *Soils and Foundations*, Vol. 47, No. 5, pp. 821-832.
- Wood, D. M. , Crewe, A., Taylor, C. 2002. “Shaking table testing of geotechnical models.”*Int J Phys Modell Geotech* 1, pp.1–13.